ELSEVIER

Tectonophysics 276 (1997) 229–251

TECTONOPHYSICS

The tectono-metamorphic evolution of gneiss complexes in the Middle Urals, Russia: a reappraisal

H.P. Echtler [a,*], K.S. Ivanov [b], Y.L. Ronkin [b], L.A. Karsten [b], R. Hetzel [a], A.G. Noskov [b]

[a] *GeoForschungsZentrum Potsdam, Telegrafenberg C2, 14473 Potsdam, Germany*
[b] *Institute for Geochemistry and Geology, Russian Academy of Sciences, Pochtovy Per. 7, Yekaterinburg 620151, Russia*

Received 14 May 1996; accepted 27 November 1996

Abstract

The Middle Urals are characterized by a major virgation in the linear trend of the Urals orogen, and represent the most highly contracted part of the late Palaeozoic collisional belt. This part of the orogen is dominated by metamorphic complexes and major fault and shear zones. The Main Uralian Fault zone (MUF), the east-dipping suture of the orogen containing low-grade metamorphic rocks, separates the Sysert Complex in the east from the Ufaley Complex in the west. The Sysert Complex in the hanging wall of the MUF consists of intensely deformed gneisses, granitic intrusions and a metamorphosed mélange zone. Tectonic and isotopic investigations suggest the following stages for the evolution of the Sysert Complex: (a) pre-orogenic rifting and magmatism during Ordovician and Silurian times; (b) oceanic closure, island arc formation related to convergence and subduction during Devonian times; (c) major ductile deformation under amphibolite facies conditions related to NW-directed thrusting associated with crustal stacking during collision in Carboniferous times; (d) exhumation and contractional intracontinental tectonics during Permian times; and (e) closing of isotope systems related to cooling and the end of orogenic shortening through Triassic times. The Ufaley Complex, in the footwall of the MUF, is interpreted as an east-dipping crustal stack that records an amphibolite facies Uralian metamorphism. Lithologically the complex can be divided into pre-orogenic European basement (West Ufaley) and intensely deformed Palaeozoic metasediments and amphibolites (East Ufaley). High-pressure relics in the East Ufaley Complex are interpreted to be the result of subduction, whereas intense ductile deformation is related to overthrusting onto West Ufaley. The West Ufaley Complex is composed of gneisses, amphibolites, migmatites and granitic intrusions and has been thrust onto Devonian limestones along a major shear zone. In both Sysert and Ufaley Complexes, NW-trending stretching lineations and top-to-the-NW kinematic indicators suggest an oblique plate convergence with a significant sinistral component. The MUF is interpreted as a major normal fault that developed congruent with continental subduction and that compensated lithospheric thickening and the rapid exhumation of subducted crust in the footwall.

Keywords: Middle Urals; tectono-metamorphic evolution; structural geology; petrology; geochronology

* Corresponding author. Fax: +49 331 288-1370. E-mail: helle@gfz-potsdam.de

PII S0040-1951(97)00058-9

1. Introduction

The Uralian orogenic belt, extending for about 2500 km north–south along strike, originated during the collision of the East European platform with a Siberian–Kasakian terrane assemblage in the late Palaeozoic (Fig. 1). The origin of the Urals in a plate tectonic framework has been discussed since the 1970's (Hamilton, 1970; Peive et al., 1977; Zonenshain et al., 1984) and is now widely accepted (e.g., Zonenshain et al., 1990; Puchkov, 1993; Matte et al., 1993). The Main Uralian Fault (MUF) represents a well-preserved plate boundary dipping to the east along most of its length. West of this suture, a west-vergent fold and thrust belt is developed within the passive margin sequence of the East European platform and the foreland basin. The eastern hanging wall is built by longitudinally continuous oceanic, island-arc, and back-arc domains constituting the Magnitogorsk Zone in the southern and the Tagil Zone in the northern Urals (Fig. 1). The MUF is characterised by an up to 20 km wide zone of tectonic mélange containing elements of continental slope, island arc and oceanic formations.

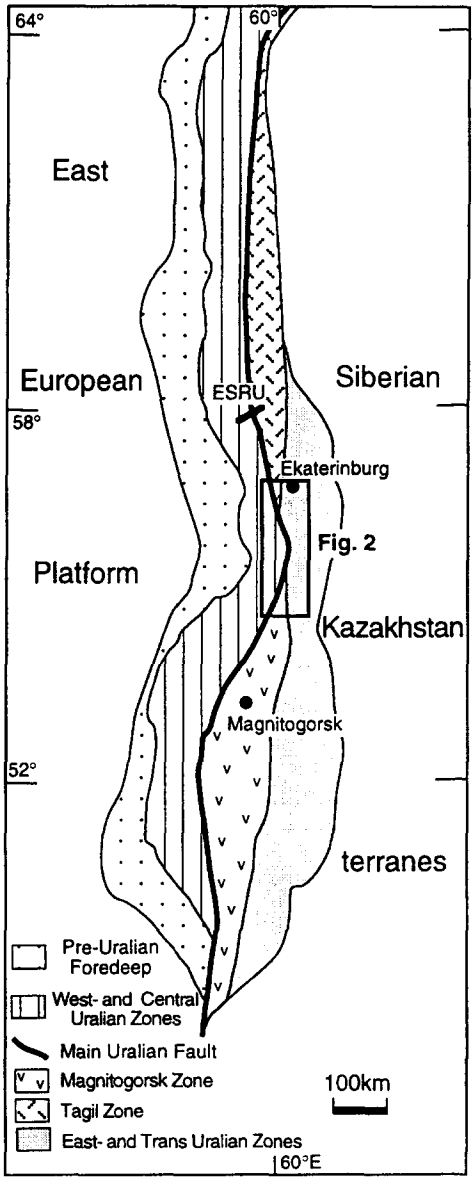

Fig. 1. Schematic tectonic map of the Urals (after Ivanov and Rusin, 1986).

The Middle Urals (between ~55° and 59°N, Ivanov et al., 1975) are characterized by a major deviation in the linear trend of the Uralian orogen, related to an East European indenter active during the late-orogenic evolution. As a consequence, this part of the collisional belt experienced the greatest contraction such that oceanic and arc domains are absent or greatly shortened in the MUF (Fig. 1).

The Middle Urals are dominated by several metamorphic gneiss complexes that were previously considered as Proterozoic continental basement underlying the Palaeozoic eugeosynclinal formations of the Urals (e.g., Keilman, 1974; Zoloev et al., 1981). The gneiss complexes were interpreted as Proterozoic blocks that experienced amphibolite to granulite facies metamorphism during the Proterozoic and greenschist to amphibolite facies metamorphism during Palaeozoic time (e.g., Keilman, 1974) or one pre-tectonic high-T metamorphism during a Palaeozoic thermal event (Ronkin et al., 1993). The present study focuses on the tectono-metamorphic evolution of the Sysert and Ufaley Complexes, two relatively well-studied examples of such metamorphic complexes, located east and west of the Main Uralian Fault, respectively (Fig. 1). Our results contradict previous models that envisioned a major pre-Palaeozoic history with static metamorphism and tectonism for these complexes. We emphasize the importance of the late Palaeozoic tectono-metamorphic history related to subduction and collisional processes.

The study is based on a 3-year collaboration be-

tween the Institute for Geology and Geochemistry (Russian Academy of Sciences, Ekaterinburg, Russia) and the GeoForschungsZentrum in Potsdam, Germany. We give an overview of a large set of existing data by integrating the results of our structural, petrographic and isotopic investigations, we develop a revised geodynamic model which should provide a basis for future research and a better understanding of the Uralian orogen.

2. Sysert Complex

The Sysert Complex forms the northern part of the Sysert–Ilmenogorsk anticlinorium, an elongate metamorphic complex which belongs to the East Uralian Zone (Fig. 2). Situated east of the MUF, this complex is composed of two large-scale, north–south-trending antiforms, the Itkul antiform in the west and the Okunkul antiform in the east (Fig. 3). The Sysert Complex was subdivided into a large number of formations (e.g., Keilman, 1974; Parnachev et al., 1986; Raevski and Parnachev, 1988); however, we here introduce a simple subdivision of two main formations: the Shumikhin and Chernov (terms adopted and redefined from Keilman, 1974). The Shumikhin formation is exposed in the cores of these antiforms (Fig. 3) and is structurally overlain by the Chernov formation. The Shumikhin formation consists mainly of orthogneisses with plagiogneisses and subordinate amounts of migmatites and rare amphibolites. The plagiogneisses have a rather consistent composition and contain mainly quartz, plagioclase, biotite and minor muscovite and garnet. The Chernov formation is composed of paragneisses with graphitic quartzites and amphibole- and/or garnet-bearing mica-schists that have been interpreted as metavolcanic rocks (Keilman, 1974). Similar lithologies at lower metamorphic grade are exposed east of the Sysert–Ilmenogorsk anticlinorium and contain fossils indicating an early to middle Palaeozoic age (Turbanov et al., 1971; Puchkov and Ivanov, 1987). Despite a major difference in metamorphic grade and their separation by a major fault they were inferred to point to similar protolith ages for the rocks of the Sysert Complex (Plusnin et al., 1965). The Chernov formation forms a metamorphosed mélange zone containing basic and ultrabasic rocks, with elongated bodies of intensely deformed gabbro, amphibolite, and serpentinite which have been collectively interpreted as an ophiolitic suite (Keilman, 1974). Granodioritic and granitic intrusive rocks are also characteristic for the complex (Fig. 3).

The evolution of the Sysert Complex has usually been related to static metamorphism and doming, and the classic concept of a mantled gneiss dome generated during Proterozoic time was widely accepted (e.g., Keilman, 1974). In this scenario a granulitic core (Shumikhin formation) was subsequently overprinted by amphibolite facies metamorphism together with the sedimentary and volcanic cover (Chernov formation) and interpreted as Proterozoic ophiolitic suites (Raevski and Parnachev, 1988). Greenschist to lower amphibolite metamorphism in the early Palaeozoic schist rim, granitization and the tectonics of the Sysert Complex were associated with long-lasting thermal diapirism and vertical movements (Keilman, 1974). Based on petrographic and geochronologic investigations Ronkin et al. (1993) and Rusin and Noskov (1993) suggested an alternative model which emphasized the absence of granulitic relics and related a pre-tectonic high-temperature metamorphism with a Lower Carboniferous thermal event (see below), associated with the intrusion of orogenic granites.

2.1. Structural geology

Structural field investigations and deformation analysis emphasize intense synmetamorphic (amphibolite facies) deformation and polyphase tectonics during the evolution of the complex. The different lithologies show a pervasive approximately N–S-trending tectonic foliation that defines two elongate antiforms (Fig. 3). Between the Itkul antiform in the west and the Okunkul antiform in the east, a N–S-trending tectonic meta-mélange zone contains intensely deformed, elongate lenses of ultrabasites, basites and granitic gneisses in a matrix of schists and quartzites. The large-scale antiformal folding postdates the ductile deformation in the Sysert Complex and is associated with late cataclastic deformation and steep, east-dipping fault zones (Fig. 3). The foliation planes are associated with a consistently NW–SE-plunging stretching lineation. Isoclinal folds at the dm-scale are common and have axes

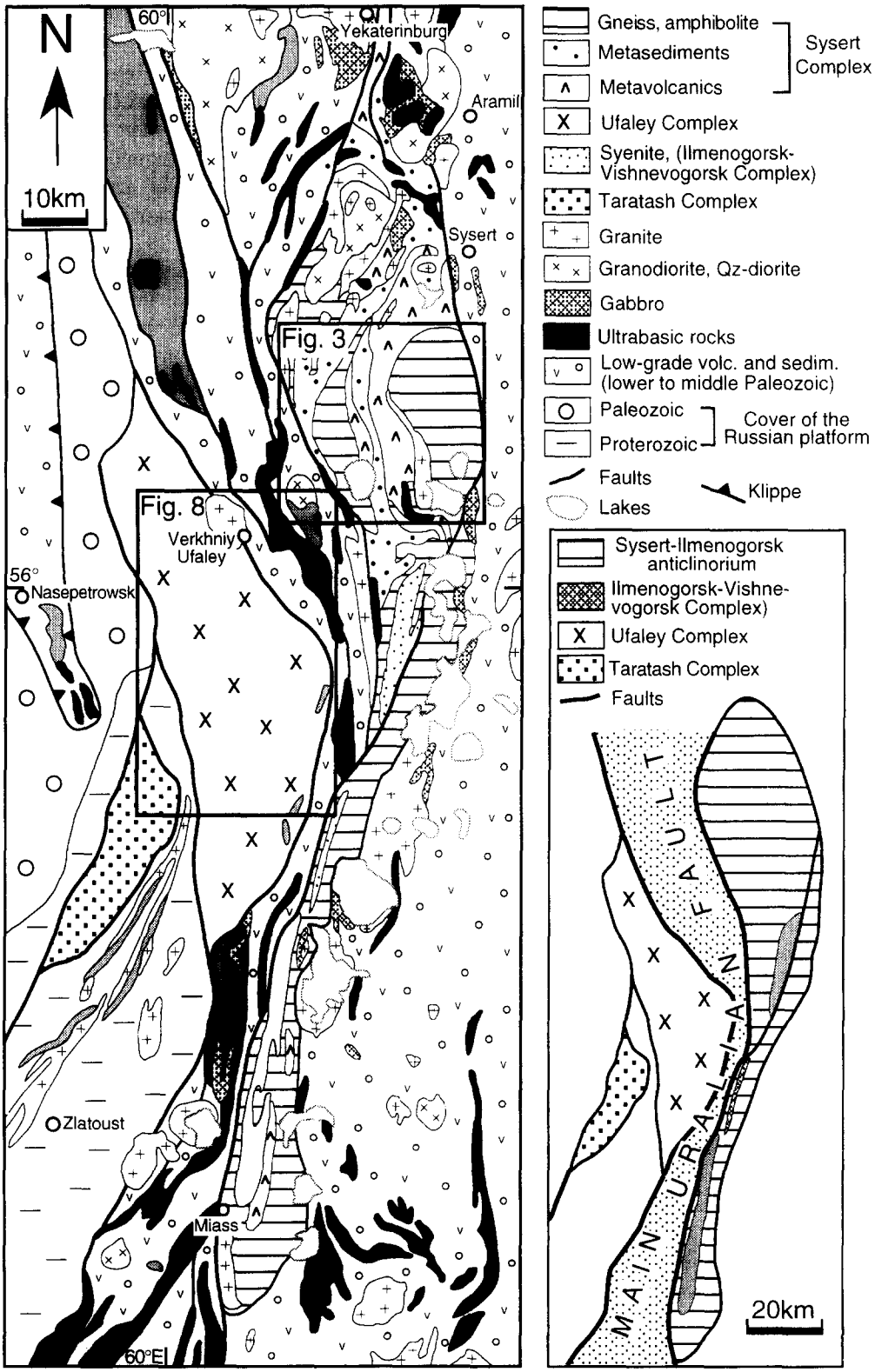

Fig. 2. Simplified geologic map of the Middle Urals after Sobolev (1986). Map at lower right shows the same area as the main figure and delineates the metamorphic complexes and the Main Uralian Fault in a schematic way.

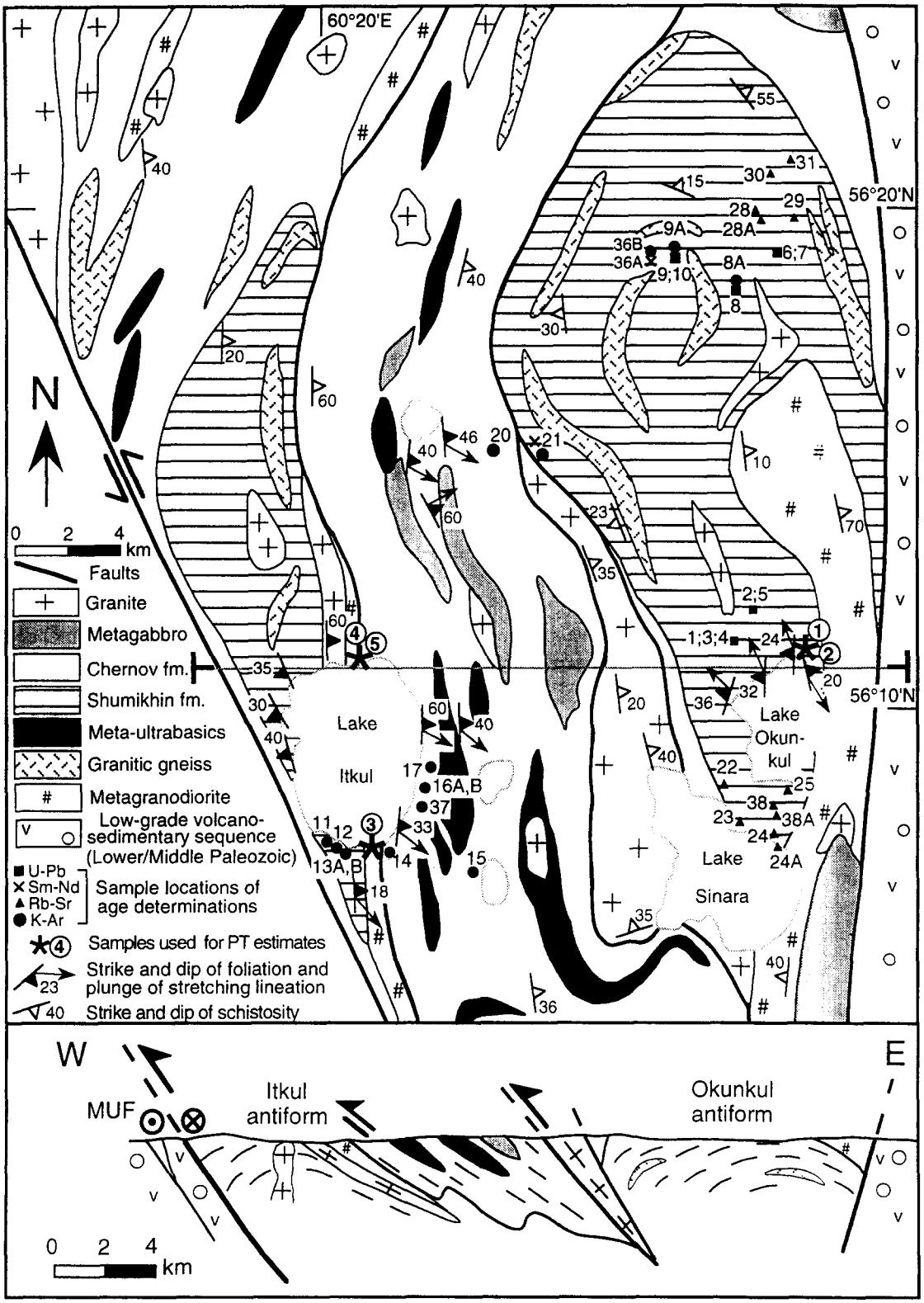

Fig. 3. Simplified geological map of the central Sysert–Ilmenogorsk anticlinorium after the 1:200,000 geological map of Keilman (1974) and own observations. Numbers at the sample locations of U–Pb samples indicate the zircon fractions shown in the concordia plot of Fig. 5.

subparallel to the stretching lineation indicating an intense ductile deformation. A number of granite and metagranodiorite bodies occur in both the Shumikhin and Chernov formations and range from very little to intensely deformed. Where present, the foliation trends subparallel to the foliation in the host rocks and stretching lineations show geometries in accordance with the regional trend.

The foliation is usually defined by a preferred shape orientation of micas and layers with different amounts of quartz and feldspar. Stretching lineations are defined by oriented micas, amphibole and elongated quartz/feldspar aggregates. Locally quartz shows serrated grain boundaries, bulging and undulose extinction indicating dynamic recrystallization. More commonly, however, quartz is relatively coarse-grained and shows slightly curved grain boundaries as a result of post-tectonic recrystallization and grain growth. Furthermore, the random orientation of amphiboles in some mica-schists indicates post-kinematic mineral growth at still elevated temperatures. Shear sense indicators have only rarely been observed in the field and in oriented thin sections, but include sigmoidal quartz–feldspar aggregates, asymmetric extensional shear bands and relics of an oblique grain-shape fabric in quartz layers (Fig. 4). The observed kinematic indicators in mylonitic domains show a consistent top-to-the-NW shear sense. The lack of abundant shear sense indicators may at least partly be the result of the post-tectonic recrystallization (Fig. 4). In general, amphibolite facies conditions during ductile deformation are suggested by the recrystallization of K-feldspar, the stability of biotite along the shear bands and the relatively large grain size of quartz.

2.2. Metamorphic petrology

The *P–T* estimates for the Okunkul and Itkul antiforms presented are based on the study of thin sections, microprobe analyses and geothermobarometry. All mineral compositions for *P–T* estimates were analyzed at the GFZ Potsdam on a CAMECA SX 100 electron beam microprobe operating in the wavelength-dispersive mode with the following conditions: 15 kV accelerating voltage, 20 nA beam current, 20 s peak counting time and 5 mm beam diameter (10 mm for white mica). CAMECA standard set was used for calibration and the PAP program for matrix correction. Representative microprobe analyses are presented in Table 1 and the sample locations are shown in Fig. 3.

The eastern Okunkul domain recorded metamorphic temperature conditions near the transition from amphibolite to granulite facies at medium pressures as indicated by the first appearance of Ca-pyroxene in garnet–clinopyroxene–andesine lenses in graphite-bearing gneisses (e.g., Keilman, 1974). The transition is accompanied by partial melting in water-bearing gneisses and illustrated by migmatitic textures, with leucosomes comprising locally 30 to 90% of the rock volume. The typical paragenesis found in leucosomes with migmatitic and granitic gneisses is garnet–biotite–muscovite–plagioclase–quartz–microcline±amphibole with veins of fresh microcline, albite–oligoclase and quartz. In the melanosomes, the typical paragenesis consists of amphibole (hastingsite or hornblende), garnet, biotite and andesine. Early garnet associated with amphibole shows a pronounced retrogressive zonation, with decreasing MgO and increasing MnO contents towards the rim. In amphibole-bearing rocks, Mg contents in garnet do not exceed 2–3% (Pyr 8–11%), whereas in migmatites without amphibole, Mg-contents are higher and reach 5–5.5% (Pyr 19–22%). Biotite is partly overgrowing amphibole and early garnets. Biotite, albite, muscovite and secondary spessartine-rich and colourless garnet crystallized from the migmatitic melt in leucosomes. Biotite locally forms inclusions in secondary garnets.

P–T estimates based on geothermobarometry give temperatures in the range of 650°–700°C and pressures of 6–8 kbar (Table 2). Studies on the stability field of hastingsite (Veblen and Ribbe, 1982) in combination with our microbe data suggest an upper temperature limit of ~750°C. Metamorphic assemblages in the western Itkul antiform indicate lower-temperature but higher-pressure conditions, compared to the Okunkul antiform. A widespread paragenesis is amphibole–plagioclase–biotite±garnet±epidote. The prograde path is illustrated by prograde zoning in garnet (decreasing MnO and increasing FeO and MgO contents towards the rim), epidote inclusions in amphibole porphyroblasts and the gradual replacement of epi-

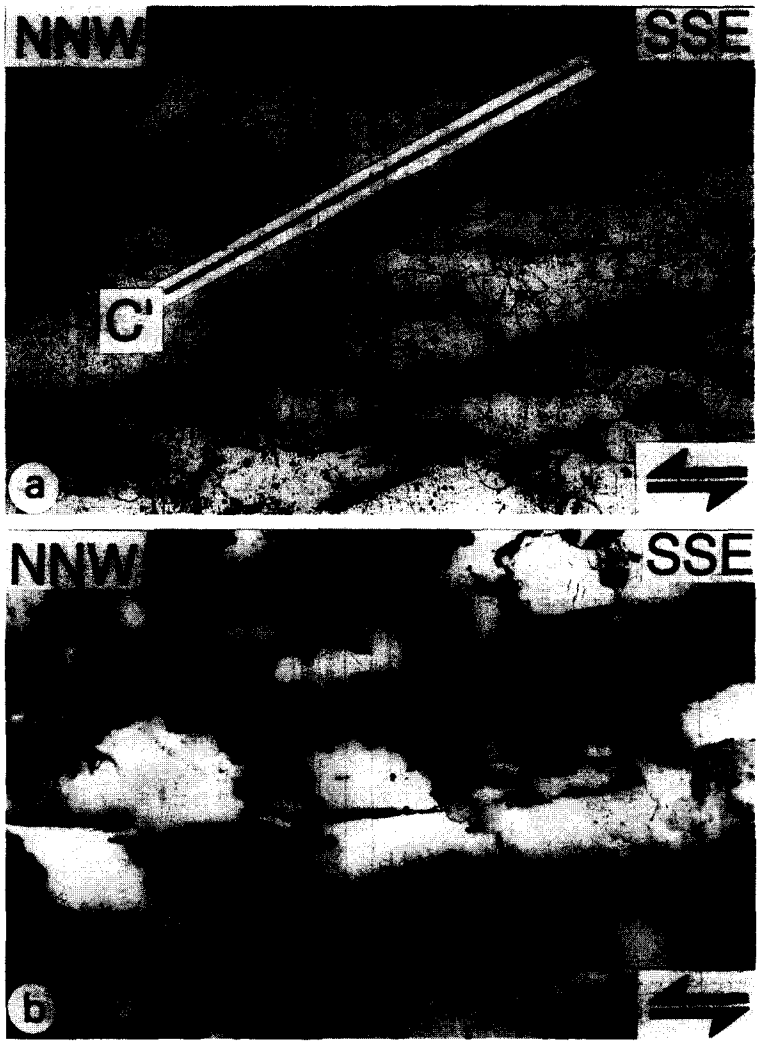

Fig. 4. Photomicrographs from the Sysert Complex. (a) Gneiss from the Shumikhin formation (northern shore of Lake Okunkul). The main foliation is defined by the preferred orientation of grain boundaries (horizontal in photomicrograph). A narrow zone dipping gently from upper left to lower right corner of the photomicrograph is defined by abundant biotite and is interpreted as a relictic shear band (*C'*). The pronounced static recrystallization overprinting the deformation structure is interpreted as a result of metamorphism outlasting deformation. Shear sense is top-to-the-NNW. Plane-polarized light. Width of photomicrograph is 5 mm. (b) Quartz-rich layer in a gneiss from the Sysert Complex (Shumikhin formation; northern shore of Lake Okunkul). The main foliation is defined by mica flakes (horizontal in photomicrograph). An oblique grain-shape fabric is defined by the preferred orientation of quartz grain boundaries, dipping from upper right to lower left at an angle of ~45° to the main foliation, and indicates a top-to-the-NNW shear sense. Plane-polarized light. Width of photomicrograph is 2.5 mm.

dote by garnet and amphibole in the matrix. Peak metamorphic conditions are represented by a relatively high tschermakite component in amphibole and high contents of Al and Ti in coexisting biotite. Retrograde metamorphism formed muscovite and chlorite. The meta-ultrabasic rocks of the Chernov formation consist of antophyllite- and actinolite-schists, that are commonly associated with talc–serpentinite±chlorite and carbonate-rich rocks that formed under decreasing *P–T* conditions and fluid interaction. *P–T* estimates obtained from the northern and southern shore of Lake Itkul suggest pressures of 7 to 10 kbar and temperatures of 500 to 600°C (Table 2).

Table 1
Representative microprobe analyses from the Sysert and Ufaley Complexes (sample locations are shown in Figs. 3 and 8)

	Shumikhin formation (Okunkul antiform)													Chernov formation		
	leucosome (1)				melanosome (2)				metagranitoid. (3)			metagranitoid. (4)		metabasite (5)		
	garnet	biotite	microcl.	plag.	garnet	amph.	plag.	biotite	biotite	amph.	plag.	garnet	amph.	garnet	biotite	amph.
Sysert Complex																
SiO_2	37.02	35.48	64.41	61.75	37.87	39.88	60.06	36.15	37.53	42.23	64.21	37.39	43.35	37.34	36.47	42.49
TiO_2	0.01	3.56			0.09	0.78		2.83	2.08	0.43		0.07	0.54	0.10	1.44	0.36
Al_2O_3	20.17	15.53	18.38	24.02	20.32	12.96	25.24	15.57	16.23	15.60	22.23	20.45	14.23	21.26	18.93	17.18
FeO	21.25	22.43	0.04		20.59	21.50		21.75	16.50	15.89		28.80	15.97	26.07	19.43	18.95
MgO	1.35	8.78			1.61	6.97		9.35	13.94	13.94		3.36	10.40	0.32	11.49	7.26
MnO	11.57	0.56			9.69	1.22		0.78	0.23	0.23		3.99	0.30	5.79	0.18	0.19
CaO	8.74		0.04	5.49	10.63	11.10	6.99	0.01	0.05	0.05	3.45	5.92	10.40	8.42		9.61
Na_2O	0.03	0.07	1.03	8.44	0.04	1.45	7.65	0.06	0.17	0.17	9.81	0.03	2.11	0.09	0.18	1.89
K_2O		9.48	15.09	0.30		1.72	0.13	9.49	8.60	8.60	0.06		0.28		8.37	0.40
Total	100.50	95.89	99.00	100.00	100.84	97.58	100.07	95.99	95.13	97.34	99.77	100.01	97.58	99.39	96.49	98.33
Si	2.99	2.74	3.00	2.75	3.00	6.21	2.67	2.78	2.80	6.30	2.84	2.98	6.29	2.72	6.30	3.01
Ti	0.001			0.21	0.005	0.09		0.16	0.11	0.05		0.004	0.06	0.08	0.04	0.006
Al IV		1.26	1.01	1.25	1.89	1.79	1.32	1.22	1.20	1.70	1.16	1.92	1.71	1.28	1.70	2.00
Al VI	1.92			0.16		0.59		0.19	0.23	1.04			0.72	0.38	1.30	
Fe	1.43			1.45	1.36	2.80		1.40	1.03	1.98		1.92	1.94	1.21	2.35	1.76
Mg	0.016			1.01	0.19	1.62		1.07	1.55	2.05		0.40	2.25	1.28	1.61	0.04
Mn	0.79			0.04	0.65	0.16		0.05	0.02	0.08		0.27	0.04	0.01	0.02	0.40
Ca	0.76	0.26	0.002		0.90	1.85	0.33	0.001	0.004	1.71	0.16	0.51	1.62		1.53	0.73
Na	0.005	0.73	0.09	0.01	0.006	0.44	0.66	0.009	0.03	0.64	0.84	0.005	0.59	0.03	0.54	0.014
K		0.02	0.90	0.94		0.34	0.007	0.93	0.82	0.08	0.003		0.28	0.80	0.08	

	metabasite (6)			grt–mica schist (7)		grt–mica schist (8)			metabasite (9)			grt–mica schist (10)			am–schist (11)	
	grt–core	grt–rim	amph.	garnet	phengite	garnet	phengite	biotite	grt–core	grt–rim	amph.	garnet	amph.	biotite	am.–core	am.–rim
Ufaley Complex																
SiO_2	37.27	37.34	44.88	36.99	52.94	37.11	51.79	38.89	37.71	37.63	42.82	37.47	40.37	35.91	44.85	49.59
TiO_2	0.12	0.04	0.33	0.16	0.21	0.03	0.21	1.55	0.04	0.05	0.51	0.05	0.68	1.88	0.19	0.20
Al_2O_3	21.70	21.97	15.32	20.63	27.23	20.90	30.73	19.47	21.03	21.09	16.12	21.66	15.07	15.21	12.59	7.42
FeO	27.88	27.43	13.75	18.70	0.65	27.75	1.41	15.16	30.55	29.02	15.34	29.50	21.46	23.42	14.38	12.21
MgO	2.40	3.21	9.31	2.96	4.47	3.92	2.84	11.39	3.27	2.80	9.42	0.53	6.11	9.07	11.30	14.13
MnO	2.20	1.57	0.18	17.69	0.12	4.70		0.32	1.80	1.38	0.06	0.55			0.23	0.18
CaO	7.73	7.68	11.65	3.16		4.85		0.16	6.14	8.13	11.26	10.06	10.26	0.03	11.91	12.13
Na_2O	0.18	0.09	1.93	0.01	0.44	0.09	0.40	0.10	0.03	0.03	2.12	0.15	2.46	0.22	1.89	1.24
K_2O			0.26		9.37		8.31	8.63			0.46		1.11	9.26	0.40	0.24
Total	99.48	99.33	97.61	100.3	95.43	99.35	95.69	95.67	100.57	100.13	98.11	99.97	97.52	95.00	97.75	97.65
Si	2.99	3.01	6.58	2.98	3.47	2.98	3.37	2.85	2.98	2.98	6.25	3.00	6.12	2.81	6.56	7.15
Ti	0.007	0.002	0.04	0.01	0.01	0.002	0.01	0.09	0.002	0.003	0.06	0.003	0.08	0.11	0.02	0.02
Al IV	2.02	2.05	1.42	1.96	0.54	1.99	0.64	1.15	1.97	1.98	1.75	2.01	1.88	1.19	1.44	0.85
Al VI			1.22		1.57		1.72	0.53			1.02		0.82	0.21	0.73	0.41
Fe	1.89	1.82	1.69	1.26	0.04	1.86	0.08	0.93	2.02	1.92	1.87	1.97	2.72	1.53	1.76	1.47
Mg	0.29	0.38	2.03	0.36	0.44	0.47	0.28	1.24	0.39	0.33	2.05	0.06	1.38	1.06	2.46	3.04
Mn	0.15	0.11	0.02	1.21	0.007	0.32		0.02	0.12	0.09	0.007	0.04			0.03	0.02
Ca	0.66	0.65	1.83	0.27		0.42		0.01	0.52	0.69	1.76	0.86	1.67	0.003	1.87	1.87
Na	0.028	0.014	0.55	0.002	0.06	0.01	0.05	0.01	0.03	0.005	0.60	0.02	0.72	0.03	0.54	0.35
K			0.05		0.78		0.69	0.81			0.09		0.22	0.92	0.08	0.04

Table 2
Calculated *P–T* conditions for the Sysert and Ufaley Complexes

Sample type	*P–T* conditions	Reference
SYSERT COMPLEX		
Eastern Ogunkul domain		
Garnet–magnesiohastingsite	*T* 662 ± 50°C	(Wells, 1979)
	T 654°C	(Lavrenteva and Perchuk, 1989)
	T 707 ± 50°C	(Powell, 1985)
Garnet (rim)–biotite	*T* 695–702°C	(Hodges and Spear, 1982)
Garnet–biotite in leucosomes	*T* 668°C	(Lavrenteva and Perchuk, 1989)
Hornblende	*P* 6 kbar	(Johnson and Rutherford, 1989)
Hornblende in leucosomes	*P* 8.1 kbar	(Hammarstrom and Zen, 1986)
Plagioclase–hornblende	*P* 7 kbar	(Fershtater, 1990)
Itkul domain		
Paragenesis epidote–biotite–Hornblende–plagioclase	*T* 513°C (*P* 7 kbar)	
	T 501°C (*P* 10 kbar)	(Spear, 1981)
Tschermakite in hornblende	*P* >7 kbar	(Veblen and Ribbe, 1982)
	P 9 kbar	(Fershtater, 1990)
	P 8 kbar, (*T* 600°C)	(Mishkin, 1990)
	P 10 kbar	(Schmidt, 1991)
Paragenesis garnet–hornblende	*T* 586°C (*P* 8 kbar)	(Wells, 1979)
	T 580°C (*P* 10 kbar)	(Wells, 1979)
	T 518°C	(Lavrenteva and Perchuk, 1989; Perchuk, 1989)
	P 8.7 ± 0.5 kbar	(Schmidt, 1991)
	P 7–8 kbar	(Fershtater, 1990; Mishkin, 1990)
UFALEY COMPLEX		
West Ufaley		
Garnet–tschermakitic hornblende	*T* 613°C	(Graham and Powell, 1984)
	T 590°C	(Powell, 1985)
	T 597 ± 50°C	(Wells, 1979)
	T 567°C	(Lavrenteva and Perchuk, 1989)
	T 550–600°C	(Lavrenteva and Perchuk, 1989)
	P 10–11 kbar	(Fershtater, 1990)
	P 11.0 ± 0.3 kbar	(Schmidt, 1991)
Garnet–biotite	*T* 578°C (with *P* 8 kbar)	(Schmidt, 1991)
	T 565°C (*P* 10 kbar)	(Lavrenteva and Perchuk, 1981)
	T 651°C	(Glebovitsky and Drugova, 1979)
East Ufaley		
Garnet–hornblende	*T* 647 ± 50°C (*P* 10 kbar)	(Wells, 1979)
	T 684°C	(Perchuk, 1981)
	T 692°C (*P* 10 kbar)	(Hodges and Spear, 1982)

2.3. Geochronology

Ub–Pb, Sm–Nd, Rb–Sr and K–Ar isotopic age determinations on samples from the Sysert Complex were performed in Ekaterinburg, Russia at the Institute of Geochemistry and Geology. The results are outlined below and the analytical procedures are described in Appendix A.

2.3.1. U–Pb results

Ten zircon fractions from five gneiss samples of the Shumikhin formation have been analysed (Table 3, Fig. 5). In general, two groups of zircons have been distinguished. Zircons of group A are commonly euhedral and long-prismatic, although some short prismatic zircons are also present. The group A zircons are interpreted to be of igneous origin. Zircons of group B are anhedral and in some cases have cores

Table 3
U–Pb isotopic data from the Shumikhin formation

Fraction	Contents (ppm)[a]		Measured isotope ratios[b]			Corrected isotope ratios[c]			Pb–Pb age (Ma)[d]
	Pb	U	$^{204}Pb/^{206}Pb$	$^{207}Pb/^{206}Pb$	$^{208}Pb/^{206}Pb$	$^{207}Pb/^{206}Pb$	$^{206}Pb/^{238}U$	$^{207}Pb/^{235}U$	
Group B									
1	44.2	1011.5	0.000736	0.06385	0.11400	0.05300	0.04250	0.3109	329 ± 19
2	39.9	901.4	0.000468	0.05966	0.11593	0.05280	0.04330	0.3153	320 ± 22
3	44.7	1015.0	0.000641	0.06267	0.11294	0.05320	0.04300	0.3160	337 ± 14
4	25.0	497.0	0.000557	0.06040	0.13972	0.05220	0.04820	0.3470	303 ± 12
5	31.3	594.4	0.000438	0.05824	0.11901	0.05180	0.05160	0.3682	277 ± 12
6	14.7	241.6	0.000725	0.06102	0.18101	0.05033	0.05600	0.3885	210 ± 16
7	10.6	168.6	0.000448	0.06014	0.21313	0.05358	0.05662	0.4184	353 ± 5
Group A									
8	23.5	345.8	0.000308	0.06011	0.12139	0.05561	0.06655	0.5102	437 ± 32
9	22.6	320.2	0.000303	0.06059	0.11468	0.05616	0.06940	0.5374	459 ± 38
10	24.1	324.3	0.000428	0.06302	0.12371	0.05677	0.07216	0.5648	482 ± 41

[a] Errors are approximately ±1%.
[b] Errors are approximately ±5% for $^{206}Pb/^{204}Pb$ and ±0.15% for $^{207}Pb/^{206}Pb$ and $^{208}Pb/^{206}Pb$.
[c] Correction: 204:206:207:208 = 1:18.23:15.639:38.178.
[d] Errors are at the 2σ level.

and show complex zoning patterns. These observations suggest that group B zircons have a metamorphic origin or have cores of group A zircons with metamorphic overgrowth. It is emphasized that all samples studied contain zircons of both groups. However, the samples from which zircon fractions 1–7 have been separated are of group B, whereas the fractions 8–10 come from samples consisting almost exclusively of zircons of group A. Zircons of group A (fractions 8–10) are slightly discordant and yield

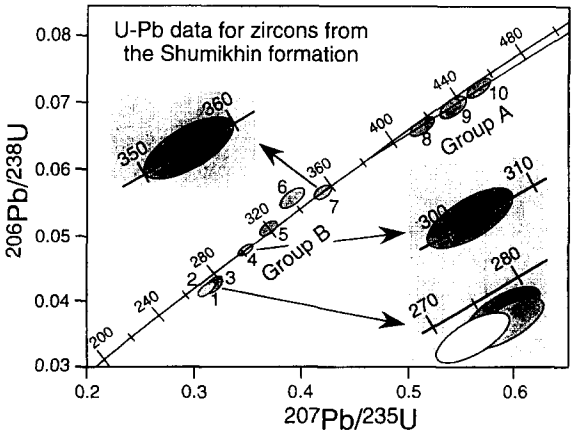

Fig. 5. U–Pb concordia diagram for the 10 zircon fraction from the Shumikhin formation.

Pb–Pb ages between 437 and 482 Ma. They define a discordia with an upper intercept at 639^{+254}_{-139} Ma and a lower intercept at 383^{+30}_{-155} Ma (95% confidence level). Zircons from samples 7 and 4 (group B) gave concordant ages of 355 ± 5 Ma and 303 ± 7 Ma. Samples 1–3 are slightly discordant and give almost identical results (Pb–Pb ages of 320 ± 22 to 337 ± 14 Ma).

2.3.2. Sm–Nd results

The results of the Sm–Nd isotopic analyses are shown in Table 4. An amphibolite (sample 36A) from the Shumikhin formation yielded a four-point mineral isochron with an age of 352 ± 40 Ma and an initial ϵ_{Nd} value of +2.1 (Fig. 6). The Sm–Nd model age for the amphibolite is 1033 Ma, whereas three other samples from the Chernov formation yield Sm–Nd model ages of 564, 600 and 807 Ma (Table 4). The four whole rock samples have present-day ϵ_{Nd} values between +5 and +7 (Table 4).

2.3.3. Rb–Sr results

Two sets of samples from the Shumikhin formation, collected from the northern and southern parts of the Okunkul antiform, were analysed for Rb–Sr isotopes. Sample locations are shown in Fig. 3 and analytical results are shown in Table 5 and illustrated in Fig. 7. Five samples of plagiogneiss from

Table 4
Sm–Nd isotopic data from the Sysert Complex

Sample	Formation	Lithology	Material	Nd (ppm)	Sm (ppm)	$^{147}Sm/^{144}Nd$ [a]	$^{143}Nd/^{144}Nd$ [b]	ϵ_{Nd} [c]	T_{DM} (Ma) [d]
36A	Shumikhin	Amphibolite	Whole rock	27.50	7.08	0.15574	0.512648	5.67	1033
			Plagioclase	2.99	0.52	0.10447	0.512529		
			Biotite	1.56	0.32	0.12581	0.512580		
			Amphibole	24.76	5.99	0.14627	0.512624		
21	Shumikhin	Am–Bio–Gneiss	Whole rock	22.28	4.71	0.12781	0.512591	6.24	807
			Biotite	2.08	0.45	0.13138	0.512698		
			Plagioclase	2.71	0.62	0.13887	0.512632		
15	Chernov	Amphibolite	Whole rock	7.71	2.17	0.16974	0.512889	6.89	564
20	Chernov	Plagioschist	Whole rock	53.20	7.57	0.08601	0.512548	6.79	600

[a] Precision of $^{147}Sm/^{144}Nd$ ratios is ±0.2% (2σ), based on analysis of standard BCR-1.
[b] Precision of $^{143}Nd/^{144}Nd$ ratios is better than 0.002% (1σ).
[c] CHUR values used in calculation are $^{147}Sm/^{144}Nd = 0.1967$ and $^{143}Nd/^{144}Nd = 0.512636$.
[d] TDM ages are calculated after method of DePaolo (1981).

the northern part of the Okunkul antiform yielded a whole-rock isochron age of 435 ± 33 Ma with an initial Sr ratio of 0.7033 ± 0.0002. Seven samples of granitic gneisses from south of Lake Okunkul gave an isochron age of 254 ± 4 Ma with an initial Sr ratio of 0.7115 ± 0.0002.

2.3.4. K–Ar results

Mineral concentrates from fifteen samples from the Shumikhin and Chernov formations have been dated with the K–Ar method, including six amphibole, nine biotite, four muscovite, and three feldspar concentrates (Table 6). The majority of the analysed samples yielded ages between 280 and 240 Ma. Two samples gave younger ages of 200 ± 5 and 205 ± 1 Ma from an undeformed dyke.

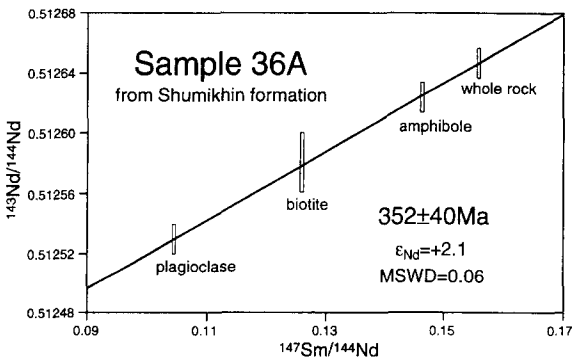

Fig. 6. Sm–Nd diagram for the samples from the Shumikhin formation.

2.3.5. Interpretation and discussion

The U–Pb data considered separately are inconclusive but maintained for discussion. The ages of the euhedral group A zircons from the metamagmatic Shumikhin formation are interpreted as protolith ages. It remains unclear whether the lower and upper intercept of the poorly defined discordia (383 + 30/ − 155 Ma and 639 + 254/ − 139 Ma) or the Pb–Pb ages (437 ± 32 to 482 ± 41 Ma) should be regarded as the formation age. The Pb–Pb ages are in agreement with the Rb–Sr whole-rock isochron age of 435 ± 33 Ma obtained from the Shumikhin formation. The Sm–Nd model ages younger or equal to 1033 Ma, the positive ϵ_{Nd} values and low initial $^{87}Sr/^{86}Sr$ ratio of about 0.7033 point to an important contribution of mantle-derived magmas during the formation of the Sysert Complex.

The group B zircons of fraction 7 gave a concordant age of 355 ± 5 Ma interpreted to date the growth of these zircons during the orogenic metamorphism. The age is in good agreement with the Sm–Nd isochron age of 352 ± 40 Ma (sample 36A) that is interpreted as the time of isotopic homogenization during the Uralian metamorphism and collision (Fig. 10b).

K–Ar analyses of amphibole and biotite from the same outcrop (sample 36B) yield ages of 283 ± 7 and 251 ± 5 Ma, respectively. Compared to the Sm–Nd age this indicates that the rocks experienced a prolonged phase of metamorphism followed by slow

Table 5
Rb–Sr isotopic data from the Shumikhin formation

Sample number	Rb (ppm)	Sr (ppm)	$^{87}Rb/^{86}Sr$ [a]	$^{87}Sr/^{86}Sr$ [b]
Granitic gneisses				
24	82.6	277.3	0.8620	0.71452
24A	74.4	231.1	0.9312	0.71501
23	94.4	167.2	1.6289	0.71728
25	98.8	100.1	2.8560	0.72202
38	160.7	116.3	3.9980	0.72571
38A	129.1	90.1	4.1195	0.72634
22	228.5	40.1	16.447	0.77104
Plagiogneisses				
29	49.5	622.4	0.2300	0.70471
28	84.6	611.6	0.4002	0.70599
28A	73.7	603.8	0.3533	0.70541
30	104.9	502.3	0.6046	0.70709
31	79.7	293.9	0.7848	0.70815

[a] 2σ error is approximately ±0.5%.
[b] 2σ error is approximately ±0.02–0.03%.

cooling. Assuming a difference of approximately 150°C between the closure temperatures of amphibole (Harrison, 1981) and biotite (Harrison et al., 1985) the cooling rate yields ~5°C Ma^{-1}. The idea of rather slow cooling is also supported by the relatively large scatter in the K–Ar ages of analysed samples (between ~290 and 240 Ma).

3. Main Uralian Fault

The MUF to the west of the Sysert Gneiss Complex (Fig. 2) is a tectonic mélange, up to 20 km wide, containing low-grade to non-metamorphic serpentinite and ultramafic sequences, marine sediments of Palaeozoic age and subordinate magmatic and metamorphic bodies. The regional trend of the MUF between the Sysert and Ufaley Complexes is NNW–SSE to N–S. Deformed rocks of the MUF commonly display a schistosity subparallel to the fault zone with intermediate dips to the east (40°–65°). The low metamorphic grade and schistose fabrics within the zone representing the serpentine fibres in foliated serpentinites locally indicate dip-slip movements. Localized zones of intense cataclastic deformation

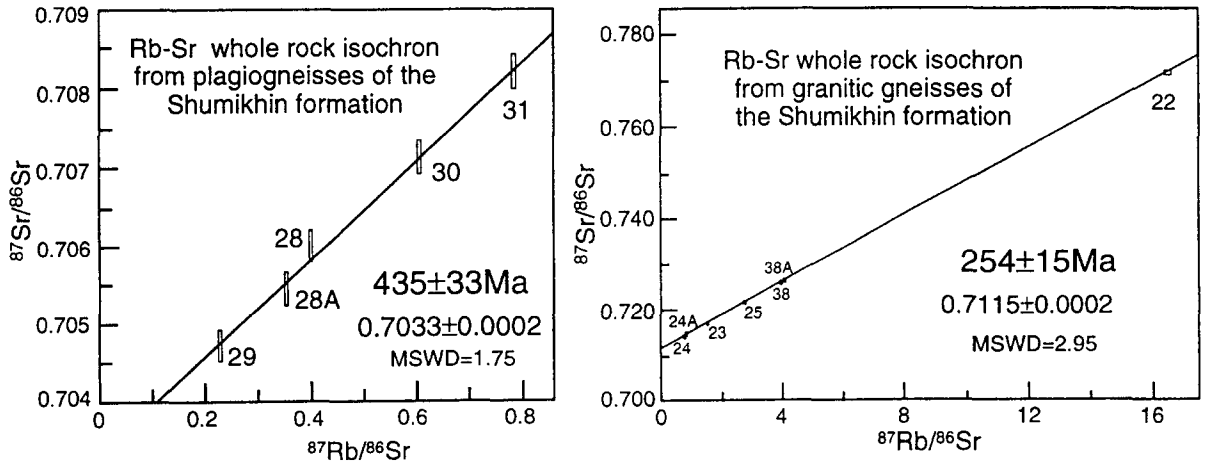

Fig. 7. Rb–Sr diagrams for the two sample sets from the Shumikhin formation.

Table 6
K–Ar isotopic data from the Sysert Complex

Sample number	Lithology	Notes	Analysed mineral	Age (Ma)
8A	Bio–gneiss	Shumikhin fm.	Biotite	291 ± 5
9A	Bio–gneiss	Shumikhin fm.	K-feldspar	240 ± 22
9A	Bio–gneiss	Shumikhin fm.	Biotite	267 ± 7
11	Plagiogranite	Dyke	Biotite	278 ± 5
12	Plagiogranite	Dyke	Muscovite	205 ± 1
13A	Plagiogneiss	Chernov fm.	Biotite	245 ± 2
13B	Plagiogranite	Dyke	Muscovite	252 ± 3
14	Amphibolite	Chernov fm.	Biotite	232 ± 1
14	Amphibolite	Chernov fm.	Amphibole	244 ± 10
15	Amphibolite	Chernov fm.	Amphibole	255 ± 9
16A	Amphibolite	Chernov fm.	Amphibole	269 ± 10
16B	Amphibolite	Chernov fm.	Amphibole	278 ± 5
17	Amphibolite	Chernov fm.	Amphibole	249 ± 4
20	Granite	Chernov fm.	K-feldspar	257 ± 25
20	Granite	Chernov fm.	Biotite	258 ± 6
20	Granite	Chernov fm.	Muscovite	262 ± 6
21	Bio–gneiss	Shumikhin fm.	Biotite	265 ± 6
21	Bio–gneiss	Shumikhin fm.	Plagioclase	271 ± 20
36B	Amphibolite	Shumikhin fm.	Biotite	251 ± 5
36B	Amphibolite	Shumikhin fm.	Amphibole	283 ± 7
37	Plagiogneiss	Chernov fm.	Biotite	200 ± 5

are steeply E-dipping to subvertical and show subhorizontal slickensides and striations. The sense of movement along these zones is commonly inferred to be sinistral on the basis of kinematic indicators. We emphasize that the deformation features described here indicate only the last increments of a complex deformation history. A detailed microtectonic analysis of the deformation in the MUF remains a target for future investigations. The moderate eastward dip of the MUF inferred from field observations is also documented by reflection seismic profiles which show the MUF as a major structure extending at least down into the middle crust (e.g., Sokolov, 1992). The ESRU profile (see Fig. 1), located at 58°N, shows the MUF as a broad band of high reflectivity dipping ~30° east, and extending to a depth of at least 12 km (i.e. 4 s TWT) (Sokolov, 1992; Juhlin et al., 1995; Steer et al., 1995).

Relics of oceanic crust and low-grade to unmetamorphosed lithologies define the structure as a major terrane boundary related to the convergence between the East European platform and outboard (including Sysert) terranes (Fig. 10). Polyphase cataclastic deformation accompanied the exhumation of the neighbouring crystalline terranes during oblique sinistral movements and major normal faulting. In the southern part of the Middle Urals, the fault zone also records a late orogenic transpressive dextral slip movement (Fig. 2) associated with the virgation and indenter tectonics.

4. Ufaley Complex

The Ufaley Complex (Fig. 8), in the footwall of the MUF (Fig. 1), is situated in the Central Uralian Zone between the MUF and the western foreland. Similar to the Sysert, the Ufaley Complex has been described as a structural dome, and subdivided into a gneissic core that experienced a pre-Palaeozoic granulite facies metamorphism (T = 750° to 900°C, P = 6 to 9 kbar), and a surrounding mantle of schists characterized by static Palaeozoic metamorphism (Keilman, 1974; Melnikov, 1976; Belkovski, 1984, 1986). The generation of rocks containing high-pressure assemblages (eclogites and kyanite schists in the eastern part of Ufaley; Kazak, 1970; Belkovski, 1986) was explained by Keilman (1974) as the result of local elevation of pressure in the contact zone between the 'gneiss core' and 'schist frame' during uplift and diapirism. Belkovski (1984, 1986) con-

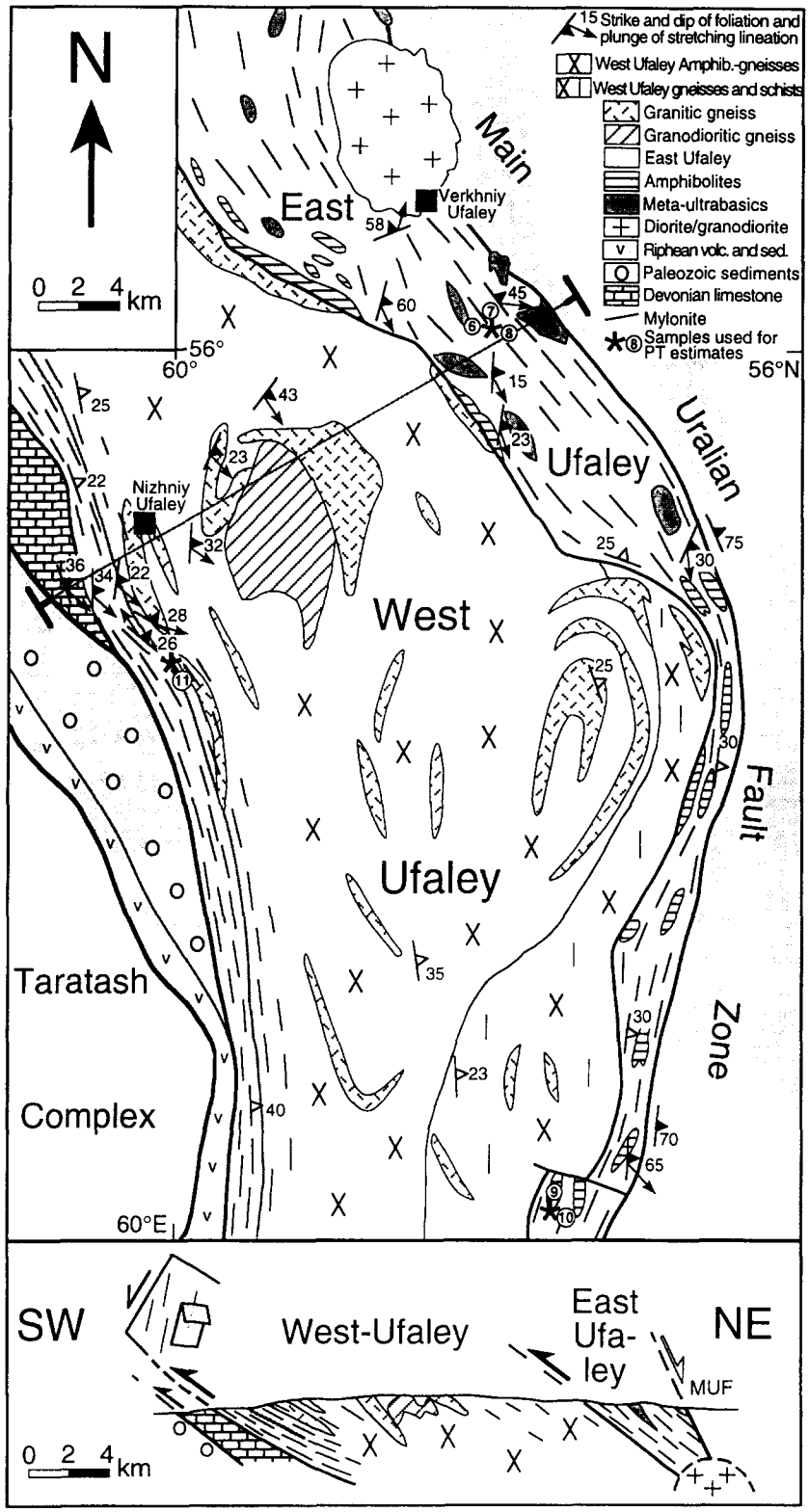
N
0 2 4 km
15 Strike and dip of foliation and plunge of stretching lineation
West Ufaley Amphib.-gneisses
West Ufaley gneisses and schists
Granitic gneiss
Granodioritic gneiss
East Ufaley
Amphibolites
Meta-ultrabasics
Diorite/granodiorite
Riphean volc. and sed.
Paleozoic sediments
Devonian limestone
Mylonite
Samples used for PT estimates
Main
East
Ufaley
Verkhniy Ufaley
Nizhniy Ufaley
West
Ufaley
Uralian
Fault
Zone
Taratash
Complex
56°
60°
56°N
60°E
SW
West-Ufaley
East Ufa-ley
NE
MUF
0 2 4 km

sidered the East Ufaley formations as pre-Riphean garnet-bearing clinopyroxenites and eclogites that formed at metamorphic conditions of 950–1200°C and 30–35 kbar, and subsequently underwent an intense metasomatism under decreasing *P–T* conditions. With the exception of abundant K–Ar age determinations (more than 100 whole-rock and mica ages; e.g., Ovchinnikov, 1963; Harris, 1977), only a few radiometric age determinations exist for the Ufaley Complex. The K–Ar ages cluster mainly between 300–400 Ma. U–Pb data on yttrium–epidote from pegmatites of the Slyudyanaya mountain yielded ages of 1470 and 1200 Ma (Mineev, 1959). These data may indicate that the Ufaley Complex represents Precambrian basement that experienced an Uralian late Palaeozoic tectono-metamorphism. Modern isotopic and radiometric analysis remains a target for future investigations.

According to Belkovski (1984), we subdivide the Ufaley Complex on the basis of lithology and metamorphic grade into East Ufaley and West Ufaley which makes up the largest part of the Ufaley Complex (Fig. 8). The East Ufaley Complex (mainly the Kurtin and Shaitan formations of Keilman, 1974) is composed of garnet mica-schists, graphitic quartzites and numerous elongate bodies of amphibolite, garnet amphibolite and lenses of ultramafic rocks (clinopyroxenite, antigorite serpentinites, talc–actinolite schists etc.). Rare bodies of eclogites have been described from the interior of large (up to several 100 m) lenses of garnet amphibolite (e.g., Kazak, 1970; Belkovski, 1986). The West Ufaley Complex is made up of plagioclase amphibolites, amphibole-bearing gneisses, migmatites, granitic gneisses and crystalline schists.

4.1. Structural geology

Rocks of the East Ufaley Complex are strongly deformed and have gently E- to SE-plunging stretching lineations (Fig. 8). Serrated grain boundaries and grain boundary bulging in quartz indicate grain boundary migration and recrystallization. Feldspars show little evidence for dynamic recrystallization. However, they often appear to be partly dissolved along contacts with muscovite grains. Numerous S–C fabrics and asymmetric pressure shadows around garnets clearly indicate a top-to-the-NW shear sense in the mica-schists (Fig. 9a). These mylonitic fabrics of the East Ufaley Complex are cross-cut by a large undeformed granodioritic intrusion near the town Verkhniy Ufaley (Fig. 8). The eastern and central parts of West Ufaley provide only poor outcrop conditions and in the high-grade metamorphic and migmatitic lithologies there are no observations of significant syn- or post-metamorphic strain. In general, the foliation within the complex dips to the east or northeast and thus contradicts the view of Keilman (1974), who described the Ufaley Complex as a structural dome. The boundary between East and West Ufaley is inferred to be a major east-dipping fault or shear zone, but was not observed in surface exposures during the course of the study (Fig. 8). The western margin of West Ufaley is marked by a major, gently (~30°) east-dipping shear zone, which is more than one kilometre thick and well-exposed southwest of the village Nizhniy Ufaley (Fig. 8). The shear zone is marked by different mylonitic fabrics which, from east to west, record decreasing metamorphic conditions. Gently dipping mylonitic foliations trend N to NW and contain mainly ESE-plunging stretching lineations (Fig. 8). Abundant shear sense indicators clearly demonstrate a top-to-the-NW movement for the shear zone (Fig. 9b–d). Approximately 2 km south of Nizhniy Ufaley, the eastern part of the shear zone is developed within intensely deformed orthogneisses and amphibole–mica-schists that were deformed under lower amphibolite/upper greenschist facies conditions (Fig. 9b). Further to the west, fine-grained metasedimentary rocks with detrital clasts of feldspar record greenschist facies conditions during deformation (Fig. 9c). The metasedimentary rocks rest on dynamically recrystallized Devonian limestones that were probably deformed at lowermost greenschist facies conditions and also contain top-to-the-NW kinematic indicators (Fig. 9d).

Fig. 8. Simplified geological map of the Ufaley Complex anticlinorium modified after the 1:200,000 geological map of Keilman (1974). Grey line along the western margin of the West Ufaley Complex indicates the approximate transition from amphibolite facies conditions in the east to greenschist facies conditions in the west.

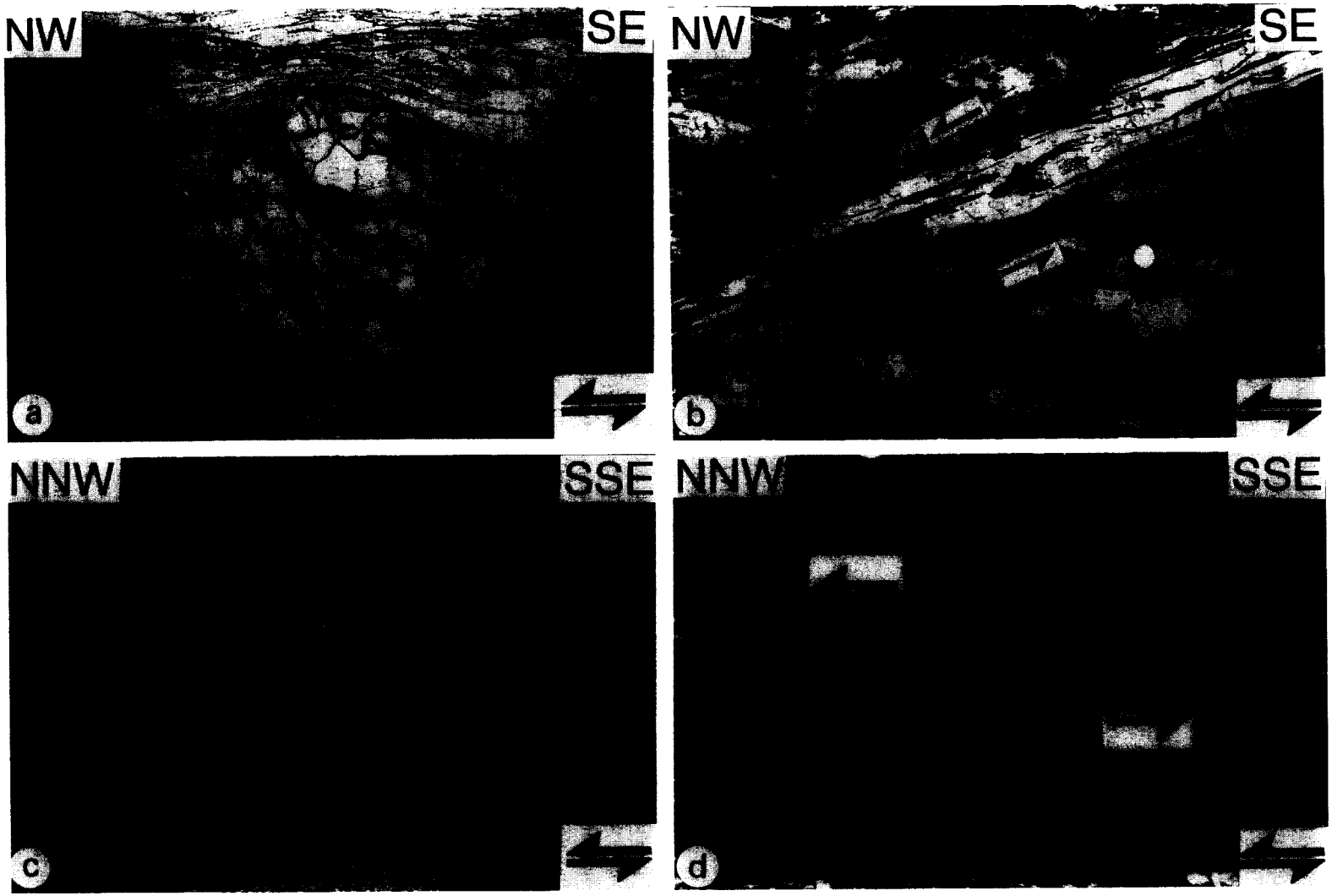

Fig. 9. Photomicrographs from the Ufaley Complex. (a) Garnet–mica-schist from eastern part of the Ufaley Complex. Garnet shows asymmetric pressure shadows consisting of quartz and chlorite. Shear sense is top-to-the-NW. Plane-polarized light. Width of photomicrograph is 10 mm. (b) Detail of asymmetric extensional shear band (from upper left to lower right) in lower amphibolite/upper greenschist facies mica-schist from the western margin of the Ufaley Complex. The schist contains epidote and amphibole. However, in the shear band only quartz and chlorite occur, probably indicating decreasing metamorphic conditions during deformation. Shear sense is top-to-the-NW. Plane-polarized light. Width of photomicrograph is 2.1 mm. (c) Metasediments from the western margin of the Ufaley Complex, deformed at lower greenschist facies conditions. Trails at upper left and lower right side of the detrital clasts consist of chlorite and quartz and indicate a top-to-the-NNW sense of shear. The detrital clasts consist of single feldspars and quartz–feldspar aggregates. Plane-polarized light. Width of photomicrograph is 5 mm. (d) Intensely deformed Devonian limestone from the western margin of the Ufaley Complex. The asymmetric shape of the σ-clast, which consists of coarse-grained calcite, indicates a top-to-the-NNW shear sense. The matrix consists of fine-grained, dynamically recrystallized calcite. Plane-polarized light. Width of photomicrograph is 2.5 mm.

4.2. Metamorphic petrology

The West Ufaley Complex shows metamorphic conditions at the transition from amphibolite to granulite facies at low to medium pressures (T = 650° to 750°C and ~4–6 kbar). This estimate is based on the paragenesis diopside–plagioclase(An_{30-50})–hornblende±garnet and the paragenesis hornblende–plagioclase(An_{25-35})–biotite–orthoamphibole (antophyllite or gedrite)±garnet (e.g., Melnikov, 1976; Bucher and Frey, 1994). Locally, retrograde greenschist facies assemblages overprint the earlier high-T parageneses and resulted in the widespread assemblage chlorite–epidote–actinolite–albite. In the shear zone along the western margin of Ufaley the amphibolite facies schist bear the assemblage epidote–albite–chlorite–amphibole. Zoned amphibole with cores of magnesio-hornblende and actinolitic rims illustrate a retrograde P–T path.

In the northern part of East Ufaley the typical paragenesis is garnet–biotite–hornblende±epidote indicating amphibolite facies conditions. The preserved prograde zonation in garnets indicates that maximum temperatures did not exceed 650°C (Tracy et al., 1976). In rare metabasite boudins, tschermakitic amphibole and garnet are interpreted as an early metamorphic paragenesis. Retrograde greenschist facies conditions are indicated by epidote–clinozoisite–chlorite assemblages that occur in both metabasites and metasediments. P–T estimates based on geothermobarometry give temperatures in the range of 560°–650°C and pressures of 10–11 kbar (Table 2).

In the southern part of East Ufaley, higher temperatures (T > 650°C) are locally indicated by the retrograde zonations of garnets and the rare presence of migmatites (Table 2). In leucosomes the presence of hastingsite and rare pargasite possibly indicate relatively high pressure (~10–12 kbar at 650°–750°C). Metamorphic conditions probably approached the transition to granulite facies under elevated pressures (Table 2).

5. Discussion and interpretation

5.1. Sysert Complex

The Sysert Complex is interpreted as a refolded and faulted mid-crustal crystalline thrust stack of Siberian affinity. According to its position in the hanging wall of the suture (MUF), it is interpreted as an above-subduction wedge buried during early Uralian (Devonian to Carboniferous) convergence. Metavolcanics and metamagmatics originated during the Ordovician to Devonian pre- to early-orogenic evolution (Fig. 10a). This period of juvenile Palaeozoic arc magmatism is also constrained by similar ages obtained from the Ilmenogorsk–Vishnevogorsk (Fig. 2) nepheline syenites located in the southern part of the Sysert–Ilmenogorsk anticlinorium (Kramm et al., 1983), where two Rb–Sr whole rock ages of 446 ± 13 Ma and 478 ± 55 Ma and a U–Pb zircon age of 434 + 15/ − 10 Ma (upper intercept of discordia) were interpreted to date the time of magma crystallization. Opening of the Uralian palaeo-ocean started in the late Arenigian (Ivanov, 1987) and consequently the radiometric age data described above are interpreted as the result of pre-orogenic rifting and magmatism between approximately 500 and 430 Ma. Further support for our interpretation comes from graptolites of Early Silurian age and conodonts of Late Silurian age that have been found in black schists in the southeastern part of the Sysert–Ilmenogorsk anticlinorium (east of Miass, Fig. 2; Plusnin et al., 1965; Puchkov and Ivanov, 1987). The only age determination that may indicate the presence of a Proterozoic crustal fragment is a single U–Pb zircon age of 1820 ± 70 Ma (upper intercept) from the southernmost part of Sysert–Ilmenogorsk (Bibikova et al., 1973), which may not be representative for the complex and should be regarded with caution. The Sm–Nd results of our study constrain that the Sysert Complex contains Proterozoic components but represents a crystalline segment that underwent to a large extent Palaeozoic metamorphic and magmatic processes. Combining the geochronological results with the tectono-metamorphic evolution strongly suggests that the main phase of deformation in the Sysert Complex is associated with the formation of the Urals and not the result of an earlier Proterozoic history.

We suggest that the major ductile deformation during NW-directed thrusting progressed with time from the higher-grade internal (eastern) to the lower-grade external (western) parts of the Sysert Complex. Westward stacking of the amphibolite facies Sysert rocks on the MUF and eastward backthrusting upon

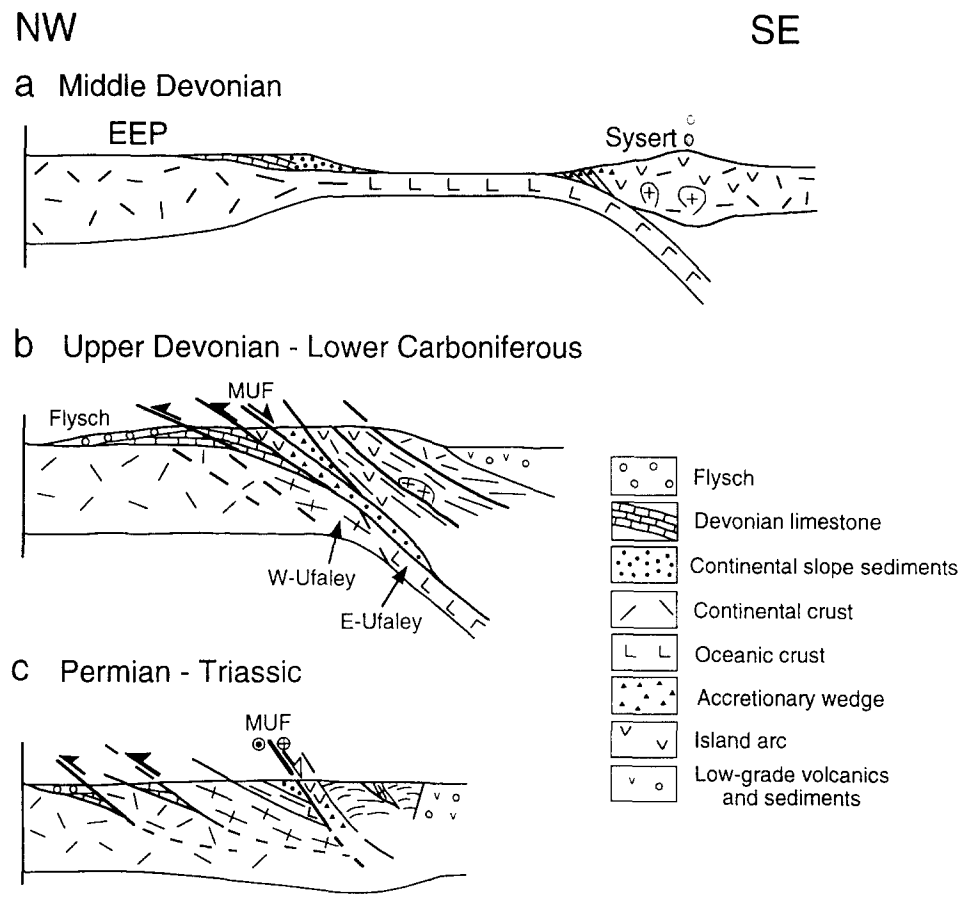

Fig. 10. Model of the Palaeozoic geodynamic and tectonic evolution in the Middle Urals. (a) Oceanic closure related to convergence and subduction during Middle Devonian times, island arc formation in a Proterozoic crustal fragment juvenated during Early Palaeozoic (Sysert); *EEP* = East European platform. (b) Continental subduction of the East European platform margin and collision, with the MUF acting as a major normal fault compensating crustal thickening. (c) Exhumation of the metamorphic Sysert and Ufaley Complexes and contractional intracontinental tectonics during Permian to Triassic times.

very low-grade formations under cataclastic conditions suggest former exhumation to a relatively shallow depth. The Itkul and Okunkul antiforms in the Sysert Complex are late features that have been formed during late-orogenic contraction, when the basement rocks where already uplifted. Instead of post-orogenic extension interpreted from seismic reflection in the Middle Urals (Steer et al., 1995) we argue for a possible syn-orogenic uplift and extension event, though not supported by our structural observations. The large-scale folding of the foliation and cataclastic faulting points to polyphase tectonics related to late-orogenic intracontinental crustal shortening. The presented K–Ar ages indicate that the rocks experienced a prolonged phase of metamorphism followed by slow cooling. This idea is also supported by the relatively large scatter between ~290 and 240 Ma. A Rb–Sr whole-rock isochron for seven samples yielded an age of 254 ± 4 Ma (Ronkin et al., 1993). Similar ages were reported from the Ilmenogorsk–Vishnevogorsk nepheline syenites where Rb–Sr mineral isochron ages of 245 ± 24 and 244 ± 8 Ma and a U–Pb age of 239 ± 40/45 Ma (lower intercept of discordia) were also interpreted to date the amphibolite facies metamorphism (Kramm et al., 1983, 1993) and are in good agreement with our results.

Widespread granitoids in the Sysert Complex and more generally in the East Uralian Zone show a late- and post-tectonic setting and can be related

to these late-orogenic processes (Fig. 10c). This is constrained by two Early Permian Rb–Sr whole-rock isochron ages (267 ± 16 Ma and 279 ± 10 Ma) obtained from the Dzhabyk granite massif located in the Southern Urals (Ivanov et al., 1995).

5.2. Ufaley Complex

In contrast to the Sysert Complex, the Ufaley Complex is not an antiformal structure but an E-dipping stack of at least two thrust sheets (West and East Ufaley). Similar to the Sysert Complex, a NW–SE-trending stretching lineation is present, which can be traced from amphibolite facies rocks in the central part of the complex to lowermost greenschist facies clastic sediments in the west. The western margin of the Ufaley Complex is bounded by a mylonitic shear zone along which it has been overthrust onto Devonian limestones, indicating that major thrusting occurred in the late Palaeozoic. This stacking in the footwall of the MUF is probably associated with the formation of the western foreland fold and thrust belt during Permian times (Brown et al., 1995).

The East Ufaley Complex is characterized by relics of high-*P*/low-*T* metamorphic assemblages, that are interpreted as the result of eastward subduction, that became part of the hanging wall by basal accretion. The high-*P* mineral associations may thus have formed as the result of prograde metamorphism of subducted basaltic and continental slope formations (Fig. 10a, b). East Ufaley is located in the northern prolongation of the Uraltau anticline and in the same structural position as the subduction-related eclogites and blueschists of the Maksyutov Complex in the Southern Urals (e.g., Dobretsov, 1974; Lennykh, 1980; Karsten and Ivanov, 1994) which have been interpreted to reflect Uralian subduction and orogeny (Ivanov, 1987). Compared to the Maksyutov the East Ufaley Complex is characterised by apparent lower metamorphic pressure, and therefore probably represents shallower fragment of the subducted slab that has been severely overprinted at amphibolite facies conditions during subsequent exhumation. The exhumation is interpreted as the result of progressive NW-directed thrusting upon the West Ufaley basement (Fig. 10c).

Shackleton and Ries (1984) suggested that regionally consistent stretching lineations across sutures in orogenic belts reflect the direction of plate motion. Together with the general north–south trend of the Uralian structures the NW–SE-trending stretching lineations and NW-directed thrusting indicate that the convergence between the East European platform and the Siberian terrane assemblage was not directed normal to the plate boundary but had an important sinistral strike-slip component. This interpretation is supported by palaeomagnetic data (Svyazhina et al., 1992).

Crustal thickness in the Middle Urals is less (~45–50 km) than north and south along strike, where a consistent orogenic root (crust up to 60 km in thickness) is preserved (Druzhinin et al., 1990). Furthermore, the West Ufaley Complex is the only East European terrane with a high-*T* remobilisation. In addition, the granite intrusions cross-cutting the MUF occur only in this part of the Urals. These unique features may be the result of regionally limited, late-orogenic re-equilibration processes in the thickened Uralian crust. The geology of the Middle Urals thus constrains to some extent the interpretation of the Uralian mountain belt as a largely preserved collisional orogen, emphasized by first interpretations of the URSEIS '95 seismic transect across the Southern Urals (Berzin et al., 1996; Carbonell et al., 1996; Echtler et al., 1996; Knapp et al., 1996).

6. Conclusions

The tectono-metamorphic evolution of the Middle Urals is related to late Palaeozoic Uralian orogenic processes with progressive east-dipping subduction and oblique northwest-directed collisional crustal stacking:

(1) The eastern Sysert Complex represents a polyphase metamorphic and magmatic history related to the Uralian orogeny. The Sysert Complex is interpreted as an above-subduction wedge of intensely deformed amphibolite/granulite facies gneisses, metavolcanic rocks, granitic intrusions and a metamorphosed mélange zone. Tectonic and isotopic investigations suggest the following stages for the evolution of the Sysert Complex: (a) pre-orogenic rifting and magmatism during Ordovician to Silurian times; (b) oceanic closure, island-arc formation related to convergence and subduction during Devonian times (Fig. 10a); (c) major ductile

deformation under amphibolite facies conditions relates to NW-directed thrusting and collisional crustal stacking during mainly Early Carboniferous times (Fig. 10b), whereas late stages are possibly associated with a subsequent exhumation event; (d) final exhumation contractional intracontinental tectonics and closing of isotope systems are related to the end of orogenic shortening until Permian to Triassic times (Fig. 10c).

(2) In both the Sysert and the Ufaley Complexes, NW-trending stretching lineations suggest an oblique plate convergence with a significant sinistral component between the East European platform and the Siberian terrane assemblage.

(3) The Ufaley Complex in the footwall of the MUF is interpreted as an east-dipping crustal stack that suffered an Uralian amphibolite facies metamorphism overprinting pre-orogenic European basement. High-pressure relics in the East Ufaley Complex are the result of subduction (Fig. 10b), whereas intense ductile deformation and inverted metamorphic sequences are related to westward overthrusting during continental subduction. Thrusting of West Ufaley onto Devonian limestones along a major shear zone (Fig. 10c) postdated amphibolite facies metamorphism and was associated with overprinting of its western margin at greenschist facies conditions.

(4) Ductile extensional deformation played only a minor role during the late-orogenic evolution. The east-dipping MUF instead truncates obliquely all lithologies and structures of the metamorphic footwall and its actual setting relates clearly to a late cataclastic normal/strike slip fault. This fault juxtaposes a very low-grade to non-metamorphic mélange with ultramafic rocks and island-arc formations upon the HP-relic bearing and medium-grade metamorphic Ufaley Complex and implies a very large displacement. The MUF is here interpreted as major normal fault that developed congruently with continental subduction (Chemenda et al., 1995) and that compensated lithospheric thickening and the rapid exhumation of subducted crust in the footwall.

Acknowledgements

This work is dedicated to the memory of A.V. Kravtsov who contributed considerably to the geochronological database of this work. We thank very much Prof. E. Bibikova, Prof. V. Koroteev, Drs. B Kaleganov, A. Rasulov, I. Pelevin and W. Seifert for supporting the investigations. We acknowledge very helpful reviews from J.N. Conelly, J.H. Knapp and Ph. Matte. The project is financed and supported by the European INTAS-project (94-1857), the Russian Science Foundation of Fundamental Investigations (94-05-16296), the German Science Foundation DFG (EC 138/3-1), the German Federal Ministry of Science and Technology (03F12GUS TP3) and the GeoForschungsZentrum Potsdam. This is EUROPROBE publication number 113.

Appendix A. Analytical procedures

U–Pb: The heavy mineral fractions of the samples were separated after crushing and using conventional heavy liquid and magnetic separation techniques. Final selection of zircons was done by hand-picking. Mineral dissolution, ion exchange column chemistry for mass spectrometer isotopic analyses were done following the procedures described by Krogh (1973) and Manhes et al. (1978). Isotopic compositions of U and Pb were measured on a CAMECA TSN solid source mass spectrometer. The total blank for Pb was approximately 20 ng for 20 mg of zircons. Common Pb corrections were done assuming Pb isotopic compositions derived from the growth curve of Stacey and Kramers (1975) using the following isotopic compositions: $^{204}Pb/^{206}Pb/^{207}Pb/^{208}Pb$ = 1/18.230/15.639/38.178. Decay constants are those recommended by Steiger and Jäger (1977).

Sm–Nd: Sample dissolution (whole rock and minerals) was done in Teflon dissolution bombs (Krogh, 1973), in a HF–HNO_3 mixture at 180°C for 24–48 h or longer when necessary, normally with aliquots of about 200 mg. For isotope dilution analyses a ^{149}Sm–^{150}Nd spike was added. Afterwards samples were dried under pure N_2, dissolved in 6 *M* HCl and dried again. The dry residue was then dissolved in 2.3 *M* HCl and placed into a centrifuge. For initial separation of the REE, a DOWEX 50 × 8 ion exchange resin column was used. Final separation of Sm and Nd was obtained with columns containing 4 cm of powdered Teflon, treated with Di-2-ethylhexyl orthophosphoric acid (HDEHP) and capped with 0.5 cm anion exchange resin. Blanks for Sm and Nd are approximately 0.2 ng and 1 ng, respectively. Isotopic compositions were measured on a FINNIGAN-MAT 262 variable multicollector mass spectrometer. Measured ratios have been normalized to a $^{146}Nd/^{144}Nd$ ratio of 0.7219. Internal statistics of the $^{146}Nd/^{144}Nd$ ratio was better than 0.0002%. Repeated runs of the La Jolla Nd standard gave a weighted mean of 0.511846 ± 0.00008 (2σ, n = 8). A ^{147}Sm decay constant of 6.54×10^{-12} and the algorithm of Ludwig (1992) were used to calculate the parameters of the Sm–Nd evolution diagram.

Rb–Sr: Rb and Sr isotopic compositions have been determined by isotope dilution. Samples were dissolved in a Teflon vessel with a mixture of HF and $HClO_4$ acids for 10 to 12 h at a temperature of 100°C and atmospheric pressure. A $^{85}Rb/^{84}Sr$ tracer was added, after the optimal sample/tracer ratio had been

estimated, based on the preliminary Rb and Sr contents of the samples obtained by X-ray fluorescence spectrometry. The dry residue was then treated with 6 *M* HCl and stored for 6 h. After drying, the residue was dissolved again in 2 *M* HCl and centrifuged. The resulting solution was loaded on a chromatographic column, 5 mm in diameter, with a 165 mm high resin layer (Bio-Rad AG50W×8 200–400 mesh). 2 *M* HCl was used as an elutant. The fraction containing Sr was evaporated and a dry residue was then passed through a column 90 mm high and 4.5 mm in diameter (Bio-Rad AG50W×8 200–400 mesh). All chemical procedures were carried out in Teflon vessels and remolten, optically transparent quartz glass. Purification of the reagents was performed by the subboiling distillation method. Typical total blanks are 0.3 ng for Sr and 0.01 ng for Rb. Isotopic analysis was performed on a modified MI-1201 mass specrometer (Ronkin, 1983). Sr in a TaF_5 solution was loaded on single W-filaments and Rb on Re–Re filaments. Fractionations were corrected by normalizing to a $^{86}Sr/^{88}Sr$ value of 0.1194. Final $^{87}Sr/^{86}Sr$ ratios have been adjusted relative to a value of 0.70800 for the Eimer and Amend $SrCO_3$ standard. Precision at the 2σ level was approximately 0.5% for $^{87}Rb/^{86}Sr$ and 0.02–0.03% for $^{87}Sr/^{86}Sr$. All ages were calculated with the regression program of Ludwig (1992), using the decay constant of 1.42×10^{-11} y^{-1} (Steiger and Jäger, 1977).

K–Ar: The concentrations of K were determined with a flame spectrophotometer and monitoring of standards. Radiogenic ^{40}Ar content was determined by a mass-spectrometric method of isotope dilution. Extraction, clearing and blending of the sample Ar with an optimum amount of ^{38}Ar tracer was produced on a metal plate. Isotopic analysis was carried out with mass spectrometers MI-1201 and MI-1330.

References

Belkovski, A.I., 1984. High pressure blastomylonites of Ufaley metamorphic block (Middle Urals). In: Magmatism and Metamorphism of Zone of Junction Between Urals and East European Platform. Sverdlovsk, pp. 42–68 (in Russian).

Belkovski, A.I., 1986. Evolution of Composition of Garnets from Eclogite–Schist and Eclogite–Schist–Migmatite Complexes. Sverdlovsk, 224 pp. (in Russian).

Berzin, R., Oncken, O., Knapp, J.H., Pérez-Estaún, A., Hismatulin, T., Yunusov, A., Lipilin, A., 1996. Orogenic evolution of the Ural Mountains: results from an integrated seismic experiment. Science 274, 220–221.

Bibikova, E.V., Gracheva, T.V., Krasnobaev, A.A., 1973. On the Belomorian phase of metamorphism in the Ilmenogorsky complex. Dokl. Akad. Nauk USSR 208, 1165–1167 (in Russian).

Brown, D., Puchkov, V., Alvarez-Marron, J., Pérez-Estaún, A., 1995. The structural architecture of the footwall to the Main Uralian Fault, southern Urals. Earth-Sci. Rev. 40, 125–147.

Bucher, K., Frey, M., 1994. Petrogenesis of Metamorphic Rocks. Springer, Heidelberg, 318 pp.

Carbonell, R., Pérez-Estaún, A., Galart, J., Diaz, J., Kashubin, S., Mechie, J., Stadtlander, R., Schulze, A., Knapp, J.H., Morozov, A., 1996. Crustal root beneath the Urals: wide-angle seismic evidence. Science 274, 222–223.

Chemenda, A.I., Mattauer, M., Malavieille, J., Bokun, A.N., 1995. A mechanism for syn-collisional rock exhumation and associated normal faulting: results from physical modelling. Earth Planet. Sci. Lett. 132, 225–232.

DePaolo, D.J., 1981. A neodymium and strontium isotope study of the Mesozoic calc-alkaline granitic batholiths of the Sierra Nevada and Peninsular ranges, California. J. Geophys. Res. 86, 10478–10488.

Dobretsov, N.L., 1974. Glaucophane Schist and Eclogite–Glaucophane–Schist Complexes of the USSR. Nauka, Novosibirsk, 429 pp. (in Russian).

Druzhinin, V.S., Egorkin, A.V., Kashubin, S.N., 1990. New data on the deep structure of the Urals and the adjacent territories by DSS data. Dokl. Akad. Nauk SSSR, 315, 5, pp. 1086–1090 (in Russian).

Echtler, H.P., Stiller, M., Steinhoff, F., Krawczyk, C., Suleimanov, A., Spiridonov, V., Knapp, J.H., Menshikov, Y., Alvarez-Marròn, J., Yunusov, N., 1996. Preserved collisional structure of the southern Urals revealed by vibroseis profiling. Science 274, 224–226.

Fershtater, G.B., 1990. Empirical hornblende–plagioclase geobarometer. Geokhimiya, 3: 328–335 (in Russian).

Glebovitsky, V.A., Drugova, G.M., 1979. Facies and subfacies boundaries for CaO-depleted rocks as defined by garnet–biotite thermo and barometry. Nauka, Contrib. Phys. Chem. Petrol. 1, 34–46 (in Russian).

Graham, C.M., Powell, R.A., 1984. Garnet–hornblende geothermometer: calibration, testing, and application to the Pelona Schist, southern California. J. Metamorph. Geol. 2, 33–42.

Hamilton, W., 1970. The Uralides and the motion of the Russian and Siberian Platforms. Geol. Soc. Am. Bull. 81, 2553–2576.

Hammarstrom, J.M., Zen, E.A., 1986. Aluminium in hornblende: an empirical igneous geobarometer. Am. Mineral. 71, 1297–1313.

Harris, M.A., 1977. Stages of Magmatism and Metamorphism During the Pre-Jurassic History of the Urals. Nauka, Moscow, 296 pp.

Harrison, T.M., 1981. Diffusion of ^{40}Ar in hornblende. Contrib. Mineral. Petrol. 78, 324–331.

Harrison, T.M., Duncan, I., McDougall, I., 1985. Diffusion of ^{40}Ar in biotite: temperature, pressure and compositional effects. Geochim. Cosmochim. Acta 49, 2461–2468.

Hodges, K.V., Spear, F.S., 1982. Geothermometry, geobarometry and the Al_2SiO_5 triple point at Mt. Moosilauke, New Hempshire. Am. Mineral. 67, 1118–1134.

Ivanov, K.S., 1987. Age of the Maksiutovo metamorphic complex of the Southern Urals. In: Metamorphic Metallogenia of the Urals. Sverdlovsk, pp. 64–67 (in Russian).

Ivanov, S.N., Rusin, A.I., 1986. Model for the evolution of the linear fold belt in the continents: example of the Urals. Tectonophysics 127, 383–397.

Ivanov, S.N., Perfiliev, A.S., Efimov, A.A., Smirnov, G.A., Necheukhin, V.M., Fershtater, G.B., 1975. Fundamental features in the structure and evolution of the Urals. Am. J. Sci. 254A, 107–136 (in Russian).

Ivanov, K.S., Ivanov, S.N., Ronkin, Y.L., 1995. On some prob-

lems of the study of orogenic granite magmatism of the Urals. In: Yearbook 1994. Ekaterinburg, 171 pp. (in Russian).

Johnson and Rutherford, 1989. Experimental calibration of the aluminium-in-hornblende geobarometer with application to the Long Valley caldera (California) volcanic rocks. Geology 17, 837–841.

Juhlin, C., Kashubin, S., Knapp, J.H., Makovsky, V., Ryberg, T., 1995. Project conducts seismic reflection profiling in the Ural Mountains. EOS, Trans. Am. Geophys. Union 76 (193), 197–198.

Karsten, L.A., Ivanov, K.S., 1994. Conditions of generation and possible diamond mineralisation in eclogites of the Urals. Dokl. Akad. Nauk USSR 335(3), 335–339 (in Russian).

Kazak, A.P., 1970. Different kind of omphacites from metamorphic rocks of South Urals. Dokl. Akad. Nauk USSR 190, 187–190 (in Russian).

Keilman, G.A., 1974. Migmatite Complexes of the Mobile Belts. Nedra, Moscow, 198 pp. (in Russian).

Knapp, J.H., Steer, D.N., Brown, L.D., Berzin, R., Suleimanov, A., Stiller, M., Lüschen, E., Brown, D.L., Bulgakov, S.N., Kashubin, S.N., Rybalka, A.V., 1996. Lithospheric scale seismic image of the southern Urals from explosive-source deep seismic reflection profiling. Science 274, 226–228.

Kramm, U., Blaxland, A.B., Kononova, V.A., Grauert, B., 1983. Origin of the Ilmenogorsk–Vishnevogorsk nepheline syenites, Urals, USSR, and their time of emplacement during the history the Ural fold belt: a Rb–Sr study. J. Geol. 91, 427–435.

Kramm, U., Chernyshev, I.V., Grauert, B., Kononova, V.A., Brücker, W., 1993. Zircon typology and U–Pb systematics: a case study of zircons from nepheline syenite of the Il'meny Mountains, Urals. Petrology 1, 474–485.

Krogh, T.E., 1973. A low contamination method for hydrothermal decomposition of zircon and extraction of U and Pb for isotopic age determinations. Geochim. Cosmochim. Acta 37, 485–494.

Lavrenteva, I.V., Perchuk, L.L., 1981. Phase correspondence in the biotite–garnet system. Experimental evidence. Dokl. Akad. Nauk, USSR 260, 731–734 (in Russian).

Lavrenteva, I.V., Perchuk, L.L., 1989. Experimental study of amphibole–garnet equilibrium (calcium-free system). Dokl. Akad. Nauk USSR 306, 173–175 (in Russian).

Lennykh, V.I., 1980. Metamorphic complexes of the Urals western slope. In: S.N. Ivanov (Ed.), Pre-Ordovician History of the Urals. Ural. Sci. Centre, Sverdlovsk, 6, 340 pp. (in Russian).

Ludwig, K.R., 1992. A plotting and regression program for radiogenic-isotopic data. U.S. Geol. Surv., Open-File Rep., 91-445: 1–40.

Manhes, G., Minster, J., Allègre, C.J., 1978. A comparative U–Th–Pb and Rb–Sr study of the Saint Severin amphoterite. Earth Planet. Sci. Lett. 39, 14–24.

Matte, P., Maluski, H., Caby, R., Nicolas, A., Kepeshinskas, P., Sobolev, S., 1993. Geodynamic model and $^{39}Ar/^{40}Ar$ dating for the generation and emplacement of the high pressure (HP) metamorphic rocks in SW Urals. C. R. Acad. Sci. Paris 317, 1667–1674.

Melnikov, E.P., 1976. *P–T* conditions of metamorphism of rocks of Ufaley gneiss complex. In: Problems of Bi-Mineral Geothermo-Barometrology. Sverdlovsk, pp. 106–126 (in Russian).

Mineev, D.A., 1959. REE-bearing epidote from pegmatites of the Middle Urals. Rep. USSR Acad. Sci., 127, N4, pp. 865–868.

Mishkin, M.A., 1990. Amphibole geotermobarometer for metabasites. Rep. Acad. Sci. USSR, 312, pp. 944–946 (in Russian).

Ovchinnikov, L.N., 1963. Isotopic age of Precambrian formations of the Urals. In: Commision on Isotopic Age Determinations of Geological Formations. Moscow, XI, pp. 235–245 (in Russian).

Parnachev, V.P., Petrov, V.I., Kuznetsov, G.P., Lukoshkov, V.N., Raevski, A.N., 1986. On structure and composition of Upper Precambrian deposits of Sysert–Ilmenogorsk zone (South Urals). In: Precambrian Volcano-Sedimentary Complexes of the Urals, pp. 9–106.

Peive, A.V., Ivanov, S.N., Necheukin, V.M., Perfiliev, A.S., Puchkov, V.N., 1977. Tectonics of the Urals. Nauka, Moscow, 120 pp. (in Russian).

Perchuk, L.L., 1981. Correction of biotite–garnet geothermometer for Mn + Mg + Fe isomorphism in garnet. Dokl. Akad. Nauk USSR, 256, pp. 441–442 (in Russian).

Perchuk, L.L., 1989. Intercorrelation of Fe–Mg geothermometers using the Nernst law. Geokhimiya 5, 611–622 (in Russian).

Plusnin, K.P., Plusnina, A.A., Zenkov, I.I., 1965. New data on graptolite schists in the Eastern slope of the South Urals. Izv. Akad. Nauk 11, 121–123 (in Russian).

Powell, R., 1985. Regression diagnostics and robust regression in geothermometer/geobarometer calibration: the garnet–clinopyroxene geothermometer revised. J. Metamorph. Geol. 3, 231–243.

Puchkov, V.N., 1993. The paleooceanic structures of the Ural Mountains. Geotectonics 27, 184–196.

Puchkov, V.N., Ivanov, K.S., 1987. On stratigraphy of black-schist formations in the East of the Urals. In: Yearbook of the Institute of Geology and Geochemistry 1986. Sverdlovsk, pp. 4–7.

Raevski, A.N., Parnachev, V.P., 1988. Structure of Itkul Section of Saitov Upper Precambrian Formation in the Middle Urals. Sverdlovsk, pp. 1–68.

Ronkin, Y.L., 1983. Modernizing of a mass-spectrometer MI-1201 used for the analysis of isotope contents of Rb and Sr. In: Methods of Isotope Geology. Acad. Sci. USSR, Moscow, 27 pp. (in Russian).

Ronkin, Y.D., Noskov, A.G., Zhuravlev, D.Z., 1993. Sm–Nd isotope system of the Sysert gneis–migmatic complex. In: Yearbook of the Institute of Geology and Geochemistry 1992. Ekaterinburg, pp. 135–139 (in Russian).

Rusin, A.I., Noskov, A.G., 1993. Composition of garnet and metamorphism of Sysert complex. In: Yearbook of the Institute of Geology and Geochemistry. Sverdlovsk, pp. 50–54 (in Russian).

Schmidt, M.W., 1991. Experimental calibration of the Al-in-hornblende geobarometer at 650°C, 3.5–13.0 kbar. Terra Abstr. 3, 30.

Shackleton, R.M., Ries, A.C., 1984. The relation between regionally consistent stretching lineations and plate motions. J. Struct. Geol. 6, 111–117.

Sobolev, I.D., 1986. Geological map of the northern, middle and northeastern part of the southern Urals. Geol. Surv. USSR and Ural Geol. Comm.

Sokolov, V.B., 1992. Crustal architecture of the Urals. Geotektonika 5, 3–19 (in Russian).

Spear, F.S., 1981. Amphibole–plagioclase equilibria: a empirical model for the relation albite + tremolite = edenite + quartz. Contrib. Mineral. Petrol. 77, 355–364.

Stacey, J.S., Kramers, J.D., 1975. Approximation of terrestrial lead isotope evolution by a two-stage model. Earth Planet. Sci. Lett. 26, 207–221.

Steer, D.N., Knapp, J.H., Brown, L.D., Rybalka, A.V., Sokolov, V.B., 1995. Crustal structure of the Middle Urals based on reprocessing of Russian seismic reflection data. Geophys. J. Int. 123, 673–682.

Steiger, R.H., Jäger, E., 1977. Subcommision on geochronology: convention on the use of decay constants in geo- and cosmochronology. Earth Planet. Sci. Lett. 36, 359–362.

Svyazhina, I.A., Puchkov, V.N., Ivanov, K.S., 1992. Reconstruction of the Ordovician Uralian Ocean based on paleomagnetic data. Geol. Geophys. XX, 17–22.

Tracy, R.J., Robinson, P., Thompson, A.B., 1976. Garnet composition and zoning in the determination of temperature and pressure of metamorphism, Central Massachusetts. Am. Mineral. 61, 762–775.

Turbanov, V.F., Pankov, Y.D., Militsina, V.S., 1971. Stratigraphy of the area of southern part of Ilmen–Vishnevogorsk anticline in connection of problem of highly metamorphosed rocks age. In: Ilmenogorsky Complex of Magmatic and Metamorphic Rocks. Sverdlovsk, pp. 23–32.

Veblen, D.R., Ribbe, P.H. (Editors), 1982. Amphiboles: Petrology and Experimental Phase Relation. Rev. Mineral. 9B, 389.

Wells, P.R.A., 1979. *P–T* conditions in the Moines of the Central Highlands, Scotland. J. Geol. Soc. London 136, 663–671.

Zoloev, K.K., Popov, B.A., Rapoport, M.S., Kontar, E.S., Levin, V.Y., 1981. Deep Structure and Metallogenia of Mobile Belts. Nedra, Moscow. 190 pp. (in Russian).

Zonenshain, L.P., Korinevsky, V.G., Kazmin, V.G., Pechersky, D.M., Khain, V.V., Matveenkov, V.V., 1984. Plate tectonic model of the South Urals development. Tectonophysics 109, 95–135.

Zonenshain, L.P., Kuzmin, M.I., Natapov, L.M., 1990. Geology of the USSR: a plate-tectonic synthesis. Am. Geophys. Union, Geodyn. Ser. 21, 242 pp.